37

FERMILAB
JUL 2 1995
LIBRARY

Fermilab Library
0 1160 0037754 3

IFT-P.021-94

IFT

Instituto de Física Teórica
Universidade Estadual Paulista

June/94

IFT-P.021/94
IFUSP/P-1111

Symmetries and time evolution in discrete phase spaces: a soluble model calculation

D. Galletti

Instituto de Física Teórica
Universidade Estadual Paulista
Rua Pamplona 145
01405-900 – São Paulo, S.P.
Brazil

and

A. F. R. de Toledo Piza

Instituto de Física
Universidade de São Paulo
Caixa Postal 20516
01452-990 – São Paulo, S.P.
Brazil

NAME	I.D. No.	M.S.

RETURN TO FERMILAB LIBRARY

Instituto de Física Teórica
Universidade Estadual Paulista
Rua Pamplona, 145
01405-900 – São Paulo, S.P.
Brazil

Telephone: 55 (11) 251-5155
Telefax: 55 (11) 288-8224
Telex: 55 (11) 31870 UJMFBR
Electronic Address: LIBRARY@IFT.UESP.ANSP.BR
47553::LIBRARY

Symmetries and Time Evolution in Discrete Phase Spaces: A Soluble Model Calculation

D. Galetti*
Instituto de Física Teórica
Universidade Estadual Paulista - UNESP
Rua Pamplona 145
01405-900 - S. Paulo - S.P. - Brazil

A. F. R. de Toledo Piza
Instituto de Física
Universidade de São Paulo
Caixa Postal 20516
01452 -990 - S.Paulo - S.P. - Brazil

May 24, 1994

Abstract

Using the flexibility and constructive definition of the Schwinger bases, we developed different mapping procedures to enhance different aspects of the dynamics and of the symmetries of an extended version of the two-level Lipkin model. The classical limits of the dynamics are discussed in connection with the different mappings. Discrete Wigner functions are also calculated.

*Partially Supported by Conselho Nacional de Desenvolvimento Científico e Tecnológico - CNPq - Brazil

1 Introduction

Phase space concepts are of fundamental importance in classical mechanics [1] and pervade quantum mechanics through the Weyl-Wigner formalism [2]. In the latter case the way in which quantum operators are mapped onto functions of pairs of classical variables while retaining all the quantum content of the original formulation was clearly established [3]. The Weyl-Wigner mapping technique has been extensively studied and discussed for the case of operators exhibiting continuous spectra [4] mainly because of relationship of the mapped expressions to their classical counterparts or classical limits. In this connection the quantum-classical correspondence was first studied in terms of a series of Poisson brackets envolving pairs of canonical variables by Moyal [5] ; the quantization was studied through an analysis of the possible link between the group of canonical transformations of classical mechanics and the unitary group of quantum mechanics in a pioneer paper by Uhlhorn [6].

In recent papers [7, 8] we have presented an alternate framework for treating the Weyl-Wigner mapping in which we can handle both continuous and discrete spectra. In this framework the Schwinger unitary operator bases [9] play an essential role as they are the building blocks for the construction of a generalized mapping kernel connecting quantum operators and functions of classical variables. The important feature in Schwinger's description is that it provides for a transparent and systematic treatment of *finite* discrete spectra, thus allowing for the possibility of including degrees of freedom without classical analogues. We have shown that it is still possible to write a Weyl-Wigner transformation and to define an equivalent discrete phase space for the associated quantum state space in such cases. To this end it was demonstrated [7] that an operator basis can be construted which will give directly the meshpoint value of the Weyl-Wigner transform of an operator by just taking its trace with the corresponding element of the basis. This basis was shown to be just the double Fourier transform of the Schwinger's original symmetrized basis and it has been used to implement the Weyl-Wigner transform both for a spin 1/2 system and for the standard, continuous canonical basis. The latter case actually involves subjecting the discrete transform to an appropriate limiting procedure. Due to its wide applicability this approach is suitable for describing the time evolution of physical quantities associated with quantum degrees of freedom which may

not have classical analogues. In this connection we have given the discrete phase space representation of the von Neumann-Liouville equation [8].

In the present paper we apply our discrete mapping technique to the study of the quantum dynamics of a soluble spin model as well as its classical limit. The model consists of a slight generalization of the well known Lipkin model [10], used many times as a testing ground for many-body approximation techniques. Special attention is given to the role of a discrete symmetry of the model (the parity symmettry of the standard Lipkin model) in shaping phase space representatives as well as the classical limit. We also study the initial value problem for some particular types of initial conditions.

In section 2 we briefly review the relevant steps of our discrete phase space mapping procedure and collect the expressions relevant for the study of the initial condition problem. Our extended version of the Lipkin model is defined in section 3. Two different realizations of the phase space mapping are introduced in subsection 3.1 and the corresponding classical limits are discussed in subsections 3.2 and 3.3. In subsections 3.4 and 3.5 we discuss constants of motion and initial value problem respectively. Finally, in section 4 we present our conclusions.

2 Brief Review

As has been pointed out previously [7, 8], it is possible to obtain the mapped representatives of quantum operators **O** , acting on finite N-dimensional spaces, through a discrete Weyl-Wigner transformation (hereafter $\hbar = 1$ unless explicitly stated)

$$O(m,n) = \frac{1}{N} Tr[\mathbf{G}^{\dagger}(m,n)\mathbf{O}] \ . \tag{1}$$

Here **G**(m,n) is the mod N invariant operator basis [8]

$$\mathbf{G}\,(m,n) = \sum_j \sum_l \frac{\mathbf{S}(j,l)}{N^{\frac{1}{2}}} \exp[i\pi\phi(j,l;N) - 2\pi\frac{i}{N}(mj+nl)] \ . \tag{2}$$

where **S**(j,*l*) is the symmetrized operator

$$\mathbf{S}(j,l) = \frac{\mathbf{U}^j\mathbf{V}^l}{N^{\frac{1}{2}}} \exp(i\pi\frac{jl}{N}). \tag{3}$$

The Schwinger unitary operators **U** and **V** are defined as [9]

$$\mathbf{U} \mid u_k\rangle = u_k \mid u_k\rangle \tag{4}$$

$$u_k = \exp(2\pi i\frac{k}{N}) \tag{5}$$

$$\mathbf{V} \mid u_k\rangle = \mid u_{k-1}\rangle \tag{6}$$

$$\mathbf{U} \mid v_l\rangle = \mid v_{l+1}\rangle \tag{7}$$

$$\mathbf{V} \mid v_k\rangle = v_k \mid v_k\rangle \tag{8}$$

$$v_k = \exp(2\pi i\frac{k}{N}) \tag{9}$$

and the two sets of eigenvectors are related by the Fourier coefficients

$$\langle u_k \mid v_l\rangle = \frac{\exp(2\pi i\frac{kl}{N})}{N^{\frac{1}{2}}} \ . \tag{10}$$

The phase

$$\phi(m,n;N) = NI_m^N I_n^N - mI_n^N - nI_m^N \ . \tag{11}$$

where I_x^N is the integral part of x with respect to N, guarantees mod N invariance. Using these expressions, it is straightforward to obtain the discrete Weyl-Wigner transform of any given state. When this state is expressed in terms of the basis $\{\mid u_k\rangle\}$, i.e.,

$$\mid a\rangle = \sum_k a_k \mid u_k\rangle \ , \tag{12}$$

a simple calculation gives in fact

$$N \cdot a_w(m,n) = Tr[\mathbf{G}^{\dagger}(m,n) \mid a\rangle\langle a \mid] =$$

$$= \frac{1}{N^{\frac{1}{2}}} \sum_{j,l} \exp[\frac{2\pi}{N} i(mj+nl) - i\pi\phi(j,l;N)]\ r(j,l) \tag{13}$$

with

$$r(j,l) = \frac{1}{N^{\frac{1}{2}}} \sum_p a^*_{\{p+l\}}\, a_p \exp[-\frac{2\pi i}{N} j(p+\frac{l}{2})] \,. \tag{14}$$

where the index $\{p+l\}$ denotes the value of the sum $p+l$ cyclicaly confined to the adopted range of index values (e.g. $p_{\max}+1 = p_{\min}$). Note that the $(p+\frac{l}{2})$ factor in the exponent must be treated as a phase, not as indicative of the need of mid-point rules (see e.g. [11]) in calculating Weyl-Wigner transforms. It should be remarked that the transforms $a_w(m,n)$ constructed in this way are in general complex-valued. In order to obtain real-valued transforms the ranges of the dummy variables j, l and p should be chosen to be symmetric about zero. Thus, for odd N, the ranges should be $-\frac{N-1}{2} \leq j, l, p \leq \frac{N-1}{2}$. This choice corresponds to the usual definition of the continuous Weyl transform (see e.g. eq.(3.8) of [7]). In this case one has explicitly

$$\{p+l\} = p + l - N I^N_{p+l+\frac{N-1}{2}} \,. \tag{15}$$

It may also be noted that the mod N phase $\phi(m,n;N)$ plays no role in the above evaluation of Wigner transforms in view of the restrictions imposed on the ranges of the various interesting discrete variables. It acquires however a crucial role when one deals e.g. with transforms of operator products or commutators, as recalled below.

The discrete phase space mapped expression for the commutator of two operators has been shown to read [8]

$$([\mathbf{O}_1, \mathbf{O}_2])(u,v) = \sum_{m,n,r,s} \sum_{a,b,c,d} \Gamma(m,n,r,s,a,b,c,d;u,v,N)$$
$$\times \{\exp[i\frac{\pi}{N}(bc-ad)] - \exp[-i\frac{\pi}{N}(bc-ad)]\} \tag{16}$$

with

$$\Gamma(m,n,r,s,a,b,c,d;u,v,N) = \frac{O_1(m,n)O_2(r,s)}{N^4} \exp[i\pi\Phi(a,b,c,d;N)]$$
$$\times \exp\{2\pi\frac{i}{N}[a(u-m)+b(v-n)+c(v-m)+d(s-n)]\} \tag{17}$$

and

$$\Phi(a,b,c,d;N) = -\phi(a+c, b+d; N) \,. \tag{18}$$

These results allow us to directly apply the mapping technique in particular to the von Neumann-Liouville time evolution equation for the density operator. In this way we find that

$$i\frac{\partial\rho}{\partial t} = [\mathbf{H}, \rho] \tag{19}$$

is mapped onto

$$i\frac{\partial\rho_w(u,v)}{\partial t} = \sum_{r,s} \mathcal{L}(u,v,r,s;N)\rho_w(r,s) \,, \tag{20}$$

where $\rho_w(r,s)$ is the mapped expression of the density operator, which is the discrete Wigner function associated to ρ and $\mathcal{L}(u,v,r,s;N)$ is the phase space discrete equivalent to the Liouville operator $\mathbf{L}$ which is written as

$$\mathcal{L}(u,v,r,s;N) = \sum_{m,n} \sum_{a,b,c,d} \frac{h(m,n)}{N^4} \{\exp[i\frac{\pi}{N}(bc-ad)] - \exp[-i\frac{\pi}{N}(bc-ad)]\}$$

$$\times \exp[i\pi\Phi(a,b,c,d;N)] \exp\{2\pi\frac{i}{N}[a(u-m)+b(v-n)+c(u-r)+d(r-s)]\} \,. \tag{21}$$

Here $h(m,n)$ is the phase space mapped form of the Hamiltonian $\mathbf{H}$.

It is evident from (20) that the time evolution is a linear process governed by the mapped Liouville operator. The commutator of the discrete phase space representatives of $\mathbf{L}$ and ρ is then a mere composition of sums – over the sites which define the discrete phase space – of elementary products of the arrays characterizing them. Once the mapped Hamiltonian of the physical system is given, equation (20) evolves the initial state in time and the dynamics propagates the original form of the initial state density in the phase space in such a form as to preserve the symmetries it embodies.

Similarly,we can also have the Heisenberg time evolution equation for an operator

$$i\frac{\partial\mathbf{O}}{\partial t} = -[\mathbf{H}, \mathbf{O}] \tag{22}$$

mapped in an analogous form as

$$i\frac{\partial O(u,v)}{\partial t} = -\sum_{r,s} \mathcal{L}(u,v,r,s;N)O(r,s) \ . \tag{23}$$

As a by-product of these equations we can observe that the conserved quantities associated to the physical system governed by the Hamiltonian $\mathbf{H}$ can be obtained by searching for the solutions of

$$\sum_{r,s} \mathcal{L}(u,v,r,s;N)O(r,s) = 0 \ . \tag{24}$$

In particular this equation is satisfied by the Wigner transform of the densities associated to each of the eigenstates of $\mathbf{H}$.

3 The extended Lipkin model

We now apply the above scheme to a spin model which extends somewhat the well known Lipkin model of nuclear physics [10]. The basic point of the extension we consider here is to explore features related to the well known "parity" symmetry of this model both in the phase-space picture of the quantum dynamics and in its classical limit. The Hamiltonian of our version of the Lipkin model is expressed in terms of a triplet of $SU(2)$ generators $\{\mathbf{S}_1, \mathbf{S}_2, \mathbf{S}_3\}$ as

$$H = \mathbf{S}_3 \cos\alpha + \mathbf{S}_1 \sin\alpha + \frac{f}{2S}\mathbf{S}_3^2 + \left[\frac{g_e + g_o}{2S} + (-1)^{S_3}\frac{g_e - g_o}{2S}\right](\mathbf{S}_1^2 - \mathbf{S}_2^2) \ . \tag{25}$$

This Hamiltonian can be diagonalized numerically within each finite S-multiplet, which accounts for the soluble character of the associated quantum dynamical problem. In addition to this general "rotational" symmetry, when $\alpha = 0$ one gets a second constant of motion which can be written as the "parity" operator

$$P = \exp(i\pi\mathbf{S}_3) \ . \tag{26}$$

This additional symmetry implies that the Hamiltonian matrix reduces, in the $\mathbf{S}_3$ representation, to two disjoint pieces involving only even and odd

eigenvalues of $\mathbf{S}_3$ respectively (we assume integer S). It should be stressed that this is a typically quantum feature in the sense that it involves the discreteness of the spectrum of the action variable $\mathbf{S}_3$ in an essential way. The two, in general different, coupling constants g_e and g_o are introduced to allow for adjusting the interaction represented by the last term independently in each of these two subspaces. In the standard Lipkin model $g_e = g_o$, and although a term equivalent to the $\mathbf{S}_3^2$ term was part of the original formulation [10], the most often considered case has also $f = 0$.

When both α and f are zero, a special feature of the energy spectrum is revealed by the fact that the Hamiltonian then *anticommutes* with the unitary operator

$$\mathbf{R} = \exp(i\frac{\pi}{2}\mathbf{S}_3)\exp(i\pi\mathbf{S}_2) = \sum_{m=-S}^{S} \mid -m\rangle i^m (-1)^{S+m} \langle m \mid \ , \tag{27}$$

which corresponds to a rotation of the angular momentum quantization frame by Euler angles $(\frac{\pi}{2}, \pi, 0)$. As a result of this anticommutation property one finds that from any energy eigenvectors $\mid E_i\rangle$ with eigenvalue E_i one can obtain another eigenvector $\mathbf{R} \mid E_i\rangle$ which has eigenvalue $-E_i$. The energy spectrum is therefore symmetric about zero in this case. Note that this property no longer holds if $f \neq 0$ and/or $\alpha \neq 0$. The parity symmetry is however broken by $\alpha \neq 0$ only.

Following the usual pratice with the Lipkin model, the Hamiltonian $\mathbf{H}$ can be implemented as a many-body problem by considering $2S$ fermions in two $2S$-fold degenerate levels and writing

$$\mathbf{S}_\pm = \mathbf{S}_1 \pm i\mathbf{S}_2 = \sum_{p=1}^{2S} a^\dagger_{p,\pm 1} a_{p,\mp 1} \tag{28}$$

$$\mathbf{S}_3 = \frac{1}{2}\sum_{p=1}^{2S}(a^\dagger_{p,+1}a_{p,+1} - a^\dagger_{p,-1}a_{p,-1}) \ , \tag{29}$$

where the indices ± 1 refer to each of the two levels. Other many-body implementations of this Hamiltonian are of course possible, e.g. using Schwinger bosonic representation of the $SU(2)$ generators [12]. These implementations, together with the fact that the model is soluble, have often been explored as a toy testing ground for several many-body approximation schemes. A different use of spin models like this one has been, on the other hand, to

study connections of quantum solutions to classical limits. In this context, in particular, the standard Lipkin model is seen as rather trivial, since the phase space of its classical limit is two-dimensional. This has led in particular to the consideration of a $SU(3)$ generalization of the standard Lipkin model which has a non-integrable classical limit. We remark, however, that at least several of the usual techniques involved in obtaining the classical limits explicitly pre-empt any more detailed evaluation of classical features that may relate to symmetries like the parity symmetry of the $SU(2)$ model. A very clear example of this is the use of $SU(2)$ (or $SU(3)$ in the "three level" version of the model) coherent state averages to derive classical limits, since these coherent states explicitly and inextricably mix the invariant subspaces of $\mathbf{H}$. We show next how the discrete Wigner mapping tools reviewed in the preceding section can be used to avoid such difficulties and keep track of parity dependent properties all the way to the classical regime.

3.1 Discrete phase-space mappings of the quantum dynamics

We turn next to the task of studying the phase space mapped version $H(m,n)$ of the quantum Hamiltonian for the extended Lipkin model. In order to set the phase space we choose the common eigenvectors of $\mathbf{S}^2$ and $\mathbf{S}_z$, $\{|S,k\rangle\}, -S \leq k \leq S$ as the eigenstates $|u_k\rangle$ of the Schwinger unitary operator $\mathbf{U}$. In order to complete the definitions of $\mathbf{U}$ and hence of the quantum kinematics we choose the eigenvalues so that

$$\mathbf{U}\,|S,k\rangle = \exp(\frac{2\pi}{N}ik)\,|S,k\rangle \tag{30}$$

with $N = 2S+1$ being the total number of states in the basis. Note that this definition adopts a symmetric range for the integer k and will therefore lead to real Wigner transforms, as stated in section 2.

With this choice of kinematics we can represent the Lipkin Hamiltonian in the finite phase space through the mapping

$$S \times H(m,n) = Tr\left[\mathbf{G}^\dagger(m,n)\mathbf{H}\right] = \sum_{k=-S}^{S} \langle u_k \,|\, \mathbf{G}^\dagger(m,n)\mathbf{H} \,|\, u_k\rangle \,. \tag{31}$$

Using standard angular momentum algebra we get, after a direct calculation,

$$S \times H(m,n) = m\cos\alpha + S_1(m,n)\sin\alpha + \frac{f}{2}m^2 + [\frac{g_e+g_o}{2S} + (-1)^m\frac{g_e-g_o}{2S}]$$

$$\times\, C(m,S)\cos(\frac{4\pi n}{N})\,, \tag{32}$$

where

$$C(m;S) = \sqrt{(S+m)(S+m+1)(S-m)(S-m+1)}\,, \tag{33}$$

and

$$S_1(m,n) = \frac{1}{2N}\sum_{j,p=-S}^{S}(\{\exp\{\frac{2\pi i}{N}[j(m-p-\frac{1}{2})+n]\}\sqrt{S(S+1)-p(p+1)}$$

$$+\exp\{\frac{2\pi i}{N}[j(m-p+\frac{1}{2})-n]\}\sqrt{S(S+1)-p(p-1)}\,)\,; \tag{34}$$

note that, due to the half-integer nature of the last factor of the exponent, this expression cannot be written in closed form like the term involving $(\mathbf{S}_1^2 - \mathbf{S}_2^2)$, where integer factors lead to Kronecker deltas. It is, however, easy to see that this is a real quantity. Its numerical evaluation is straightforward for finite N, and the limiting expression for very large N can also be easily obtained in closed form as discussed in the next subsection and in the Appendix. The result of the evaluation of these expressions for a sample case is shown in figs. 1(a) (eq.(32) with $\alpha = 0$) and 2(a) (eq.(34)). The discrete Wigner transform of the ground state of the Hamiltonian shown in fig.1(a) is shown in fig.5(a).

Once we are given the mapped Hamiltonian, it is trivial to write the Liouville operator for the extended Lipkin model

$$\mathcal{L}(u,v,r,s;N) = \mathcal{L}_1(u,v,r,s;N) + \mathcal{L}_2(u,v,r,s;N)\,. \tag{35}$$

where

$$\mathcal{L}_1(u,v,r,s;N) = \sum_{a,b,c,d=-S}^{S} \sum_{m,n=-S}^{S} \frac{m\cos\alpha + \frac{J}{2S}m^2}{N^4}$$

$$\times\{\exp[i\frac{\pi}{N}(bc-ad)] - \exp[-i\frac{\pi}{N}(bc-ad)\}\exp[i\pi\Phi(a,b,c,d;N)]$$

$$\times \quad \exp\{2\pi\frac{i}{N}[a(u-m)+b(v-n)+c(u-r)+d(v-s)]\} \qquad (36)$$

is the part corresponding to the S_3-dependent term while

$$\mathcal{L}_2(u,v,r,s;N) = \frac{1}{N^4}\sum_{a,b,c,d=-S}^{S}\sum_{m,n=-S}^{S}\{[\frac{g_e+g_o}{2S} + (-1)^m\frac{g_e-g_o}{2S}]C(m;S)$$

$$+S_1(m,n)\sin\alpha\} \times \cos(4\pi\frac{n}{N})\{\exp[i\frac{\pi}{N}(bc-ad)] - \exp[-i\frac{\pi}{N}(bc-ad)]\}$$

$$\times\exp[i\pi\Phi(a,b,c,d;N)]\exp\{2\pi\frac{i}{N}[a(u-m)+b(v-n)+c(u-r)+d(v-s)]\} \qquad (37)$$

describes the interaction term.

Before turning to the discussion of large N limiting situations we consider an alternate kinematical scheme which is adapted to the cleavage imposed by the parity symmetry. We still use the states $|S,k\rangle$ as eigenstates of the $\mathbf{U}$ operator, but modify the full definition of this operator (now denoted as $\mathbf{U}_p$) by setting its eigenvalues as

$$\mathbf{U}_p\,|S,k\rangle = \exp(\frac{2\pi}{N}iv_k)\,|S,k\rangle\ . \qquad (38)$$

where the correspondence between k and the integers $-S \le v_k \le S$ is defined to be

$$k(v_k) = \left\{\begin{array}{ll} 2v_k + S & \text{for } -S \le v_k \le 0 \\ S - 2v_k + 1 & \text{for } 1 \le v_k \le S \end{array}\right. \qquad (39)$$

This implies that the two domains of v_k correspond to eigenvalues k of $\mathbf{S}_3$ of different parities. It is clear moreover that $\mathbf{U}$ and $\mathbf{U}_p$ (and therefore also $\mathbf{V}$ and the operator $\mathbf{V}_p$ corresponding to $\mathbf{U}_p$) are unitarily related via the transformation which amounts to a relabeling of the $\{|S,k\rangle\}$ basis. This procedure in fact illustrates the use of the freedom in defining the Schwinger operators $\mathbf{U}$ and $\mathbf{V}$ to adapt the quantum kinematics to possible symmetries of the problem in hand. Furthermore, implementing the general discrete mapping procedure with $\mathbf{U}_p$, $\mathbf{V}_p$ will lead to an alternate discrete phase-space description which is quantum- mechanically equivalent to that based on $\mathbf{U}$, $\mathbf{V}$ but which explicitly "unshuffles" the definite parity subspaces. Also, since the unshuffling transformation is not smooth, in the sense that eigenvectors of $\mathbf{U}$ with consecutive eigenvalues may correspond to widely separated $\mathbf{U}_p$ eigenvalues, one may expect and indeed finds radical changes in the phase-space pictures of dynamical objects in the two cases.

Let us consider then as an example the phase-space mapping of the parity-symmetric Lipkin Hamiltonian $\mathbf{H}$ (with $\alpha = 0$) in this alternate separated parities scheme. The mapping of functions of $\mathbf{S}_3$ only is straightforward since $\mathbf{S}_3$ and $\mathbf{U}_p$ are still commuting operators. One gets

$$S \times [F(\mathbf{S}_3)]_p(m,n) = F(k(m_k))\ . \qquad (40)$$

where $k(m_k)$ is the function defined in (39).

The mapping of the operators $\mathbf{S}_1^2 - \mathbf{S}_2^2 = \frac{1}{2}(\mathbf{S}_+^2 + \mathbf{S}_-^2)$ involves now sums of exponentials containing half integer factors and which therefore cannot be reduced to simple, closed expressions for finite S, but still can be easily performed numerically. One gets

$$S \times [\frac{1}{2}(\mathbf{S}_+^2 + \mathbf{S}_-^2)](m,n) = \frac{1}{2N}\sum_{j=-S}^{S}$$

$$\{\sum_{p=-S}^{0}\sqrt{2p(2p+1)(2p+2S+1)(2p+2S+2)}\exp\{\frac{2\pi i}{N}[j(m-p-\frac{1}{2})-n]\}$$

$$+\sum_{p=1}^{S}\sqrt{(2p-1)(2p-2)(2p-2S-2)(2p-2S-3)}\exp\{\frac{2\pi i}{N}[j(m-p+\frac{1}{2})+n]\}$$

$$+\sum_{p=-S}^{0}\sqrt{(2p-1)(2p-2)(2p+2S)(2p+2S-1)}\exp\{\frac{2\pi i}{N}[j(m-p+\frac{1}{2})+n]\}$$

$$+\sum_{p=1}^{S}\sqrt{2p(2p+1)(2p+2S)(2p-2S-1)}\exp\{\frac{2\pi i}{N}j[(m-p-\frac{1}{2})-n]\}\} \ . \quad (41)$$

A large N limit of this expression is also easily obtained and will be discussed in the next subsection.

Finally, we can also map the operator $\mathbf{S}_1$ in the separated parities scheme. This operator is essentially anti-diagonal and therefore strongly nonlocal in the $\mathbf{U}_p$ representation. The mapping is a straightforward algebraic exercise which gives

$$Tr[\mathbf{G}_p^\dagger(m,n)\mathbf{S}_1] = \frac{\Delta_{\{m-S-1\}}}{2}(\sum_{p=-S}^{-\frac{S+1}{2}}+\sum_{p=\frac{S+1}{2}}^{S})\sqrt{4\mid p\mid S-4p^2+2\mid p\mid}$$

$$\times\exp(-\frac{4\pi i}{N}np)+\frac{\delta_{m,0}}{2}\sum_{p=-\frac{S-1}{2}}^{\frac{S-1}{2}}\exp(-\frac{4\pi i}{N}np)\sqrt{4\mid p\mid S-4p^2+2\mid p\mid}$$

$$+\frac{\Delta_{\{m-1\}}}{2}\{\sum_{p=-\frac{S-1}{2}}^{0}\exp[-\frac{2\pi i}{N}n(2p-1)]\sqrt{4\mid p\mid -4p^2+2(S-\mid p\mid)}$$

$$+\sum_{p=1}^{\frac{S+1}{2}}\exp[-\frac{2\pi i}{N}n(2p-1)]\sqrt{4\mid p\mid S-4p^2+6\mid p\mid -2(S+1)}\}$$

$$+\frac{\delta_{m,-S}}{2}\{\sum_{p=-S}^{-\frac{S+1}{2}}\exp[-\frac{2\pi i}{N}n(2p-1)]\sqrt{4\mid p\mid S-4p^2+2(S-\mid p\mid)}$$

$$+\sum_{p=\frac{S+3}{2}}^{S}\exp[-\frac{2\pi i}{N}n(2p-1)]\sqrt{4\mid p\mid S-4p^2+6\mid p\mid -2(S+1)}\} \ . \quad (42)$$

Here Δ_k is the real function defined as (see Appendix)

$$\Delta_k = \frac{1}{N}\sum_j \exp[\frac{2\pi i}{N}j(k+\frac{1}{2})] \ . \quad (43)$$

As a practical note we mention that in order to evaluate numerically mapped operators all algebraic work can be saved by using directly the form given in equation (14). The above expression will be nevertheless useful to discuss the large N limit of the mapped $\mathbf{S}_1$ operator in the following subsection.

The result of the evaluation of these expressions for the same sample case which was taken as an illustration of the mixed parities mappings is shown in figs. 3(a) and 4(a). The discrete Wigner transform of the ground state of the Hamiltonian shown in fig. 3(a) is also shown in fig. 5(b).

3.2 Large N limit as classical limit

In this subsection we study the previously constructed mappings in the large N limit interpreted as a classical limit of the spin model. The basic procedure to be followed can be encapsulated in the formal limit

$$\lim_{S\to\infty}\frac{S}{i\hbar}[\frac{\mathbf{S}_i}{S},\frac{\mathbf{S}_j}{S}] \equiv \{s_i,s_j\} = \epsilon_{ijk}s_k \ . \quad (44)$$

where the curly brackets are to be interpreted as Poisson brackets (For finite S the spectra of the $\mathbf{S}_i/S$ are contained in the interval $(-1,1)$ and get denser as S increases while $\hbar/S$ decreases). The Hamiltonian is also scaled by S^{-1} so that, for $g_e = g_o = g$, the limiting procedure gives directly

$$H^{cl}(g_e = g_o = g) = s_3\cos\alpha + s_1\sin\alpha + \frac{f}{2}s_3^2 + g(s_1^2 - s_2^2) \ . \quad (45)$$

Using the Poisson brackets of the $\mathbf{S}_i$ one can immediately obtain classical equations of motion from which it follows that $\frac{d}{dt}\vec{S}^2 = 0$.

We now subject our mapped expressions $H(m,n)$ and $H_p(m,n)$ to this same limiting procedure. Considering first the limit of $H(m,n)/S$, and using

$$\lim_{S\to\infty} \frac{m}{S} = s_3 \tag{46}$$

and

$$\lim_{S\to\infty} 2\pi \frac{n}{N} = \varphi \ , \tag{47}$$

where now s_3 and φ are interpreted as continuous c-number variables with values in the range $(-1,1)$ and $(-\pi,\pi)$ respectively, we get

$$\lim_{S\to\infty} \frac{1}{S} H(m,n) = s_3 \cos\alpha + \lim_{S\to\infty} \frac{1}{S} S_1(m,n) \sin\alpha + \frac{f}{2} s_3^2 + g(1-s_3^2)\cos 2\varphi \ . \tag{48}$$

In order to obtain the limit of the term involving $\mathbf{S}_1$ we use the formal correspondence

$$\lim_{S\to\infty} \frac{1}{N} \sum_{j=-S}^{S} \exp[\frac{2\pi i}{N} j(m-p+\frac{1}{2})] \to \delta_{m,p} \ . \tag{49}$$

which holds when this sum occurs in connection with sufficiently smooth functions of p as is the case here (see Appendix), to obtain

$$\lim_{S\to\infty} \frac{1}{S} S_1(m,n) \sin\alpha = \sqrt{1-s_3^2}\cos\varphi \sin\alpha \ . \tag{50}$$

The resulting limit is therefore just the classical Hamiltonian H^{cl} written in terms of the *canonical* variables s_3 and φ which correspond to the projection of the unit action vector $\vec{s}$ on the 3-axis and the associated azimuthal angle respectively. The result of its numerical evaluation in a sample case is shown in fig. 1(b).

Turning next to the $\mathbf{U}_p - \mathbf{V}_p$ (separated parity) description, applying the limiting procedure also to the case $g_e = g_o = g$ but restricting ourselves first to the conserved parity Hamiltonian with $\alpha = 0$, we get

$$H_p^{cl}(g_e = g_o = g; \alpha = 0) = 1 - 2\mid\sigma\mid - 4g(\mid\sigma\mid - \sigma^2)\cos\xi + \frac{f}{2}(1-2\mid\sigma\mid)^2 \ , \tag{51}$$

where $m/S \to \sigma$ and $\frac{2\pi}{N} n \to \xi$ are the continuous classical variables in this case. The result of the numerical evaluation of this expression in a sample case is shown in fig. 3(b). It should be recalled that the sign of σ identifies the parity sector in this scheme. Reference to eq. (39) also shows that $m = 0$ belongs in fact to the sector of dimensionality $S+1$ in the finite S case. It is worth remarking that one can relate $\mathbf{H}_p$ to $\mathbf{H}$ "canonically" in a formal way by a transformation associated with the generating function [13]

$$F_2(\sigma,\varphi) = (1-2\mid\sigma\mid)(\varphi - \frac{\pi}{2}) \ , \tag{52}$$

which gives

$$s_1 = \frac{\partial F_2}{\partial \varphi} = 1 - 2\mid\sigma\mid \tag{53}$$

$$\xi = \frac{\partial F_2}{\partial \sigma} = (\pi - 2\varphi)[2\theta(\sigma) - 1] \ , \tag{54}$$

where $\theta(\sigma)$ is the usual step function defined so that $\theta(0) = 0$. It is clear however that this is not a one to one mapping of the two phase-spaces : while each value of s_3 is associated with two values of σ with opposite signs, each value of ξ (mod 2π) corresponds to two values of the azimuthal angle φ (mod 2π) which differ by π. This limitation, which in particular makes the transformation of the parity non-diagonal s_1 operator (written as $\sqrt{1-s_3^2}\cos\varphi$) completely ambiguous, can, however, be given physical content by remarking that there are two distinct limiting realizations of each value of s_3, namely involving $\mathbf{S}_3$ eigenstates of opposite parities; at the same time, in the mixed parities (i.e., $\mathbf{U}-\mathbf{V}$) representation, objects of definite parity are represented by phase-space distributions which are periodic functions of the azimuthal angle with period π. An example of this is the Hamiltonian $\mathbf{H}$ itself when $\alpha = 0$, together with the fact that its periodicity with period π is broken when $\alpha \neq 0$ (cf. fig. 2). In order to explore this complementarity of the two phase-space descriptions somewhat further one may consider also H_p^{cl} with $g_e \neq g_o$ but still with $\alpha = 0$. We get in this case (assuming odd S)

$$H_p^{cl}(\alpha = 0) = 1 - 2\mid\sigma\mid + \frac{f}{2}(1-2\mid\sigma\mid)^2 +$$

$$+ \{g_e\theta(\sigma)\sqrt{\sigma-\sigma^2} + g_o[1-\theta(\sigma)]\sqrt{-\sigma-\sigma^2}\}\cos\xi \ , \tag{55}$$

which allocates different phase-space domains to each of the now different dynamical regimes in each of the two parity sectors. These two regimes are on the other hand hopelessly shuffled in the $\mathbf{U}-\mathbf{V}$ representation. Here the discrete mapping becomes staggered on account of the interaction term

$$\frac{1}{2}[(g_e+g_o)+(-1)^m(g_e-g_o)]C(m;S) \tag{56}$$

which wildly oscillates between different levels as the classical limit is approached while still keeping the π periodicity intact when $\alpha = 0$ (see fig. 6).

We turn next to the study of the large S limit of the mapped version of $\mathbf{S}_1$ in the separated parities scheme. This is easy to obtain using eq. (42) the preceding subsection. Including the S^{-1} scaling factor one gets in the way

$$\frac{1}{S}Tr[\mathbf{G}_p^\dagger(m,n)\mathbf{S}_1] \simeq 2S(\Delta_{\{m+S\}}+\delta_{m,-S}+\Delta_{\{m-1\}}+\delta_{m,0})g_p(n)\ , \tag{57}$$

where the function Δ_k can be approximated for large S as (see Appendix)

$$\Delta_k \simeq \begin{cases} (-1)^k\dfrac{2}{(2k+1)\pi} & ,0\le k\le S \\ (-1)^{k+1}\dfrac{2}{|2k+1|\pi} & ,-S\le k\le -1 \end{cases} \tag{58}$$

and

$$g_p(n) \simeq \frac{1}{2}\int_0^1 dx\sqrt{x-x^2}\cos 2\pi n x = \begin{cases} \dfrac{\pi}{16} & ,n=0 \\ (-1)^n\dfrac{J_1(|n|\pi)}{4|n|} & ,1\le|n|\le S \end{cases} \tag{59}$$

where $J_1(x)$ is a cylindrical Bessel function. The mapped operator is therefore a staggered and increasingly singular function of m and n as S increases. The large S approximations used in deriving these analytical expressions consist in neglecting terms of the order S^{-1} or smaller in the evaluation of the

n–dependence and approximating sums by integrals (cf. the evaluation of Δ_k in the Appendix). The result of the numerical evaluation of this expression is shown in fig. 4(b).

Since $\mathbf{S}_1$ has vanishing diagonal matrix elements in the $\mathbf{S}_3$ representation, one must have

$$\lim_{S\to\infty}\sum_{n=-S}^{S} g(n) = 0\ . \tag{60}$$

Since $g(n)$ is always negative for $|n|>0$ and approaches zero rather slowly, this sum converges to zero also rather slowly as S increases. The difference between $S_1(m,n)$ evaluated (a) numerically for a finite value of S and (b) from the analytical asymptotic expression truncated at the same finite value of S are illustrated in fig. 4.

We see therefore that when the parity symmetry is broken by the $\mathbf{S}_1$ term, the mapped Hamiltonian does not have a smooth limit when the classical regime is approached. For any finite value of S it still contains, however, complete information on the quantum dynamics of the model.

3.3 Discussion

We summarize in this subsection our understanding of the general picture that emerges from the preceding analysis of the Lipkin model. The main point to be stressed is that our mapping procedure allows for a very large flexibility in the selection of the kinematical framework in which it is carried out. As illustrated by the use of the mixed parities ($\mathbf{U}-\mathbf{V}$) scheme and of the separated parities ($\mathbf{U}_p-\mathbf{V}_p$) scheme, this flexibility can in particular be explored in such a way as to lead to smooth mapped representatives of the relevant dynamical variables (e.g. the Hamiltonian). Since the different kinematical schemes are unitarily related, they all give equivalent descriptions at the quantum level. The smoothness requirement is, however, more than just a matter of convenience when one implements large N limits as classical limits of the quantum dynamics. As we have shown above, useful classical limits for the broken parity ($\alpha\neq 0$), $g_e = g_o$ case in the $\mathbf{U}-\mathbf{V}$ scheme can be obtained, but not in the $\mathbf{U}_p-\mathbf{V}_p$ scheme, since the $\mathbf{S}_1$ term becomes strongly nonlocal in the $\mathbf{U}_p$ representation. Conversely, when $\alpha = 0$ but $g_e\neq g_o$ a smooth classical limit can be obtained in the $\mathbf{U}_p-\mathbf{V}_p$ but not in

the mixed parity, $\mathbf{U}-\mathbf{V}$ scheme. In general, the (discrete) symmetries of the dynamics seem to provide for one criterion leading to useful kinematic schemes. Conversely, we may also note that through the use of symmetry adapted kinematical schemes (such as the $\mathbf{U}_p-\mathbf{V}_p$ scheme in the case of the standard form of the Lipkin model, i.e. $\alpha=0$, $f=0$ and $g_e=g_o$) the mapped dynamics assumes such a form that the existence of distinct, uncoupled sectors is explicitly manifest as a partitioning of the phase-space which holds all the way into the classical limit. In the case we studied above these phase-space sectors are identified as $\sigma\leq 0$ and $\sigma>0$ respectively in the $\mathbf{U}_p-\mathbf{V}_p$ scheme; when the $\mathbf{U}-\mathbf{V}$ scheme is adopted instead, no such partitioning survives the classical limit, and the parity symmetry manifests itself classicaly through the more subtle property of period-halving in the azimuthal angle φ.

3.4 Constants of motion

In order to look for the conserved quantities in the standard Lipkin model ($g_e=g_o=g$, $f=0$, $\alpha=0$) we must require, as already mentioned, that an equation of the type

$$\sum_{r,s=-S}^{S}\mathcal{L}(u,v,r,s;N)O(r,s)=0 \tag{61}$$

must be satisfied.

For the moment, however, let us study a particular family of conserved quantities, namely those that are function of the angular momentum only. Hence

$$\sum_{r,s=-S}^{S}\mathcal{L}(u,v,r,s;N)q(r)=0 \tag{62}$$

is the equation we have to solve. In this case, the first term in the mapped Liouvillian, $\mathcal{L}_1$, being proportional to m only, gives no contribution for any $q(r)$. The second term, $\mathcal{L}_2$, when applied to $q(r)$, gives

$$\sum_{r,s=-S}^{S}\mathcal{L}_2(u,v,r,s;N)q(r)=igC(u;S)\sin(4\pi\frac{v}{N})[q(u+1)-q(u-1)]\ . \tag{63}$$

It is then clear that any function depending solely on the angular momentum which satisfies

$$q(u+1)=q(u-1) \tag{64}$$

is a conserved quantity.

In a similar fashion one can show that for a function of the angle variable only, a more entangled equation can be obtained which characterize the corresponding associated conserved quantities, being a particular family of solutions of the form

$$\varphi(s)=\exp(4\pi i\frac{ts}{N})\ , \tag{65}$$

for any integer t. It is interesting to note that the double period in this kind solution is related to the second power of the operators $\mathbf{S}_+$ and $\mathbf{S}_-$ appearing in the Lipkin Hamiltonian which, by their turn, describe the excitation of pairs of particles between the levels.

3.5 Initial value problem

Now let us study the time evolution equation for the standard ($g_e=g_o=g$, $f=0$, $\alpha=0$) Lipkin model. To this aim, we must have the mapped expression of the density operator, so that we can solve

$$i\frac{\partial\rho_w(u,v;t)}{\partial t}=\sum_{r,s=-S}^{S}[\mathcal{L}_1(r,s,u,v)+\mathcal{L}_2(r,s,u,v)]\rho_w(r,s;t) \tag{66}$$

once the initial Wigner function $\rho_w(r,s;t=0)$ is given.

The general final expression is written in terms of the mapped Hamiltonian defining the mapping of the Liouvillian operator and one hardly could see the details of the time evolution. In order to clarify how the dynamics associated to the standard Lipkin model acts in the discrete phase space , we will study two limiting cases again, namely those in which the density depends only on the angular momentum or the phase variable respectively. In the first case we have

$$\rho=|u_j\rangle\langle u_j|\ , \tag{67}$$

being this operator mapped onto

$$\rho_w(m,n) = \delta_{m,j} \ , \tag{68}$$

that is, the density is a constant for the value j of the angular momentum and is independent of the phase variable.

Introducing this expression in (66) we note again that the first contribution, coming from the mean field term, vanishes for any function depending only on the angular momentum . The second term, associated to $\mathcal{L}_2$, gives then the final expression for the time evolution equation, for small time interval

$$\rho_w(u,v,t) \cong \delta_{u,j} + gC(u;S)\sin(4\pi\frac{v}{N})(\delta_{u,j-1} - \delta_{u,j+1})\Delta t \ . \tag{69}$$

For the case of a density associated to an angle dependent state

$$\rho = |v_l\rangle\langle v_l| \ , \tag{70}$$

it is easy to see that

$$\rho_w(m,n) = \delta_{n,l} \tag{71}$$

and that the two terms in (66) contribute to the final expression. After a direct calculation we obtain

$$\rho_w(u,v,t) \cong \delta_{n,l} - 2\sum_{m,a,d} \sin(\pi a\frac{d}{N})\frac{1}{N^2}\exp\{2\pi\frac{i}{N}[a(u-m)+d(v-l)]\}$$

$$\times \{m + \frac{g}{2}C(m;S)[\exp(4\pi i\frac{v}{N} + i\pi a I^N_{d+2}) - \exp(-4\pi i\frac{v}{N} + i\pi a I^N_{d-2})]\} \tag{72}$$

which shows the spreading of the density all over the phase space as time goes on.

4 Conclusions

We have described in detail an application of our discrete phase space mapping technique, based on the unitary operator bases proposed by Schwinger, to an extended version of the two level Lipkin model. The main point

to be stressed is that this technique allows for considerable flexibility in its implementation as a direct result of the generality and strictly constructive definition of the Schwinger bases. We made explicit use of this flexibility for developing different mapping procedures to enhance different aspects of the dynamics and of the symmetries of the model; the different procedures are unitarily related in an explicit way, and lead to quite different phase space representatives. Its usefulness is particularly clear when considering classical limits of the dynamics, as it allows for reducing the often encountered staggered behavior of the phase space representatives of quantum objects. It should also be stressed in this connection that the limiting procedure which involves increasing the dimensionality of the basic state vector space is straightforward and algebraically performed in terms of the Schwinger bases.

As a test of these features we have explicitly evaluated for the Lipkin model the mapped versions of several objects, including the Hamiltonian and its associated Liouville-von Neumann dynamical equation. Discrete Wigner functions for energy eigenstates were also calculated. The main tool involved in implementing our procedure is the construction of the appropriate operator basis, Eq.(2), in terms of which the Weyl-Wigner transforms are simply expressed in terms of the trace operation, Eq.(1). The numerical evaluation of the resulting expressions is straightforward using present computational techniques.

5 Appendix

We discuss here in some detail the evaluation of sums of the type

$$\Delta_k \equiv \frac{1}{2S+1}\sum_{j=-S}^{S}\exp[2\pi i\frac{j}{2S+1}(k+\frac{1}{2})] =$$

$$= \frac{1}{2S+1} + \frac{2}{2S+1}\sum_{j=1}^{S}\cos\frac{(2k+1)\pi}{2S+1}j \tag{73}$$

with $-S \le k \le S$ in the limit of very large values of S. The Δ_k are obviously real numbers. For very large S the sum over cosines can be approximated by an integral as

$$\frac{2}{2S+1}\sum_{j=1}^{S}\cos\frac{(2k+1)\pi}{2S+1}j \longrightarrow \frac{2}{2S+1}\frac{2S+1}{\pi}\int_0^{\frac{\pi}{2}}\cos(2k+1)\theta d\theta\ , \qquad (74)$$

where we defined the angle θ as $\pi j/(2S+1)$ and supplied the appropriate Jacobian. We obtain thus

$$\Delta_k \rightarrow \frac{2}{\mid 2k+1 \mid}\sin \mid 2k+1 \mid \frac{\pi}{2} = \begin{cases} (-1)^k \dfrac{2}{(2k+1)\pi} & , k \geq 0 \\ (-1)^{k+1}\dfrac{2}{\mid 2k+1 \mid \pi} & , k \leq -1 \end{cases} \qquad (75)$$

Furthermore one has

$$\lim_{S\rightarrow\infty}\sum_{k=-S}^{S}\Delta_k \rightarrow \frac{4}{\pi}(1-\frac{1}{3}+\frac{1}{5}-\frac{1}{7}+...) = \frac{4}{\pi}arctg1 = 1 \qquad (76)$$

so that one has, *for sufficiently smooth functions* f_k,

$$\lim_{S\rightarrow\infty}\sum_{k=-S}^{S}\Delta_k f_k \rightarrow f_0\ , \qquad (77)$$

i.e., for such functions f_k, Δ_k has a δ-function behaviour. "Sufficiently" smooth here means that f_k does not vary appreciably with k for sufficiently many values of k away from zero and is sufficiently bounded everywhere so as to guarantee the dominance of the contributions coming from the vicinity of $k=0$. This explains, in particular, why the δ-function prescription gives useful results when taking the classical limit of the spin model Hamiltonian in the $\mathbf{U}-\mathbf{V}$ (mixed parity) scheme. When the $\mathbf{S}_1$ operator is mapped in the $\mathbf{U}_p-\mathbf{V}_p$ (separated parities) scheme, one obtains contributions which are proportional to the function Δ_k and are therefore strongly staggered objects.

References

[1] V. Arnold, Mathematical Methods of Classical Mechanics (Springer Verlag, New York, 1978)

[2] E. Wigner, Phys. Rev. **40** (1932) 749; H. Weyl, The Theory of Groups and Quantum Mechanics (Dover, New York, 1950)

[3] S.R. de Groot and L.G. Suttorp, Foundations of Electrodynamics (North Holland, Amsterdam, 1972) chap. VI

[4] M. Hillery et al., Phys. Rep. **106C** (1984) 121; N.L. Balaz and B.K. Jennings, Phys. Rep. **104C** (1984) 347

[5] J.E. Moyal, Proc. Camb. Phil. Soc. **45** (1949) 99

[6] U. Uhlhorn, Arkiv för Fysik **11** (1956) 87

[7] D. Galetti and A.F.R. Toledo Piza, Physica **A149** (1988) 267

[8] D. Galetti and A.F.R. Toledo Piza, Physica **A186** (1992) 513

[9] J. Schwinger, Proc. Nat. Acad. Sci. **46** (1960) 570,893,1401; **47** (1961) 1075

[10] H. Lipkin, N. Meshkov and A. Glick, Nucl. Phys. **62** (1065) 188

[11] J. Hannay and M. Berry, Physica **D1**(1980) 267

[12] J. Schwinger, On Angular Momentum, 1951, Report U.S. AEC NYO-3071 (unpublished) (reprinted in Quantum Theory of Angular Momentum, ed. L.C. Biedenharn and H. van Dam, Academic Press, 1965)

[13] H. Goldstein, Classical Mechanics (Addison-Wesley Pub., Reading, Ma, 1970) chap. 8

6 Figure Captions

Fig. 1- (a) Discrete transform of H for S = 15; (b) Classical limit of (a) in the mixed-parities $(U - V)$ scheme. Parameters are $\alpha = f = 0$, $g_e = g_o = 2$ in both cases.

Fig. 2- (a) Discrete transform of S_1 for S = 15; (b) Classical limit of (a). In both cases the mixed-parities $(U - V)$ scheme is used. Note the absence of azimuthal period-halving for this parity non-diagonal operator.

Fig. 3- Same as Fig. 1 but using the separated-parities $(U_p - V_p)$ scheme.

Fig. 4- (a) Discrete transform of S_1 for S = 15; (b) Analytical asymptotic form for large S evaluated at S = 15. The separated-parities $(U_p - V_p)$ scheme is used.

Fig. 5- Discrete Wigner transform of the ground state wavefunctions of the Hamiltonian of figs. 1 and 3. (a): mixed-parities $(U - V)$ scheme (cf. Fig.1); (b): separated-parities $(U_p - V_p)$ scheme (cf. Fig.3).

Fig. 6- Discrete transform of H for S = 15, $\alpha = f = 0$, $g_e = 0.5$ and $g_o = 2$. (a): mixed-parities $(U - V)$ scheme; (b): separated-parities $(U_p - V_p)$ scheme.

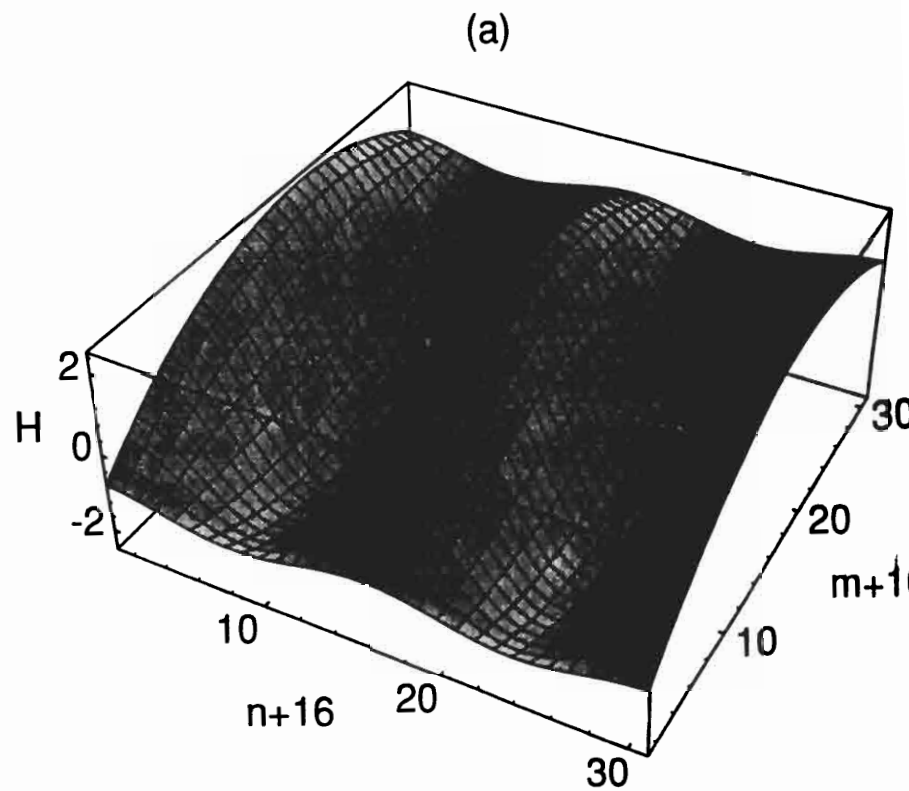

Fig. 1

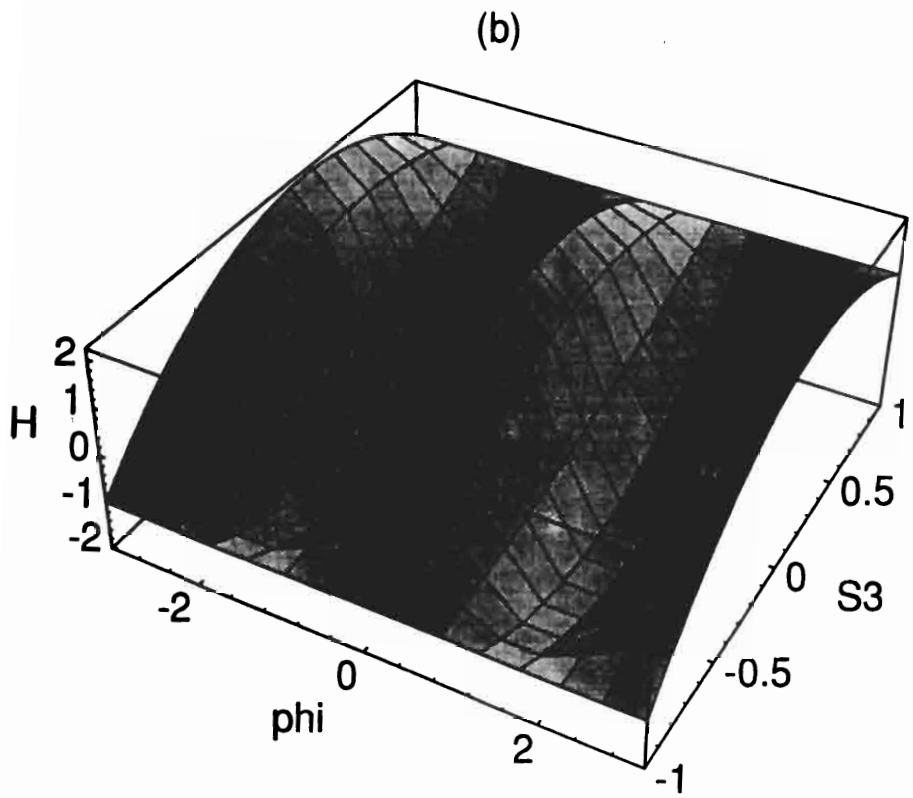
(b)
H
2
1
0
-1
-2
-2
0
phi
2
1
0.5
0
S3
-0.5
-1

Fig. 1

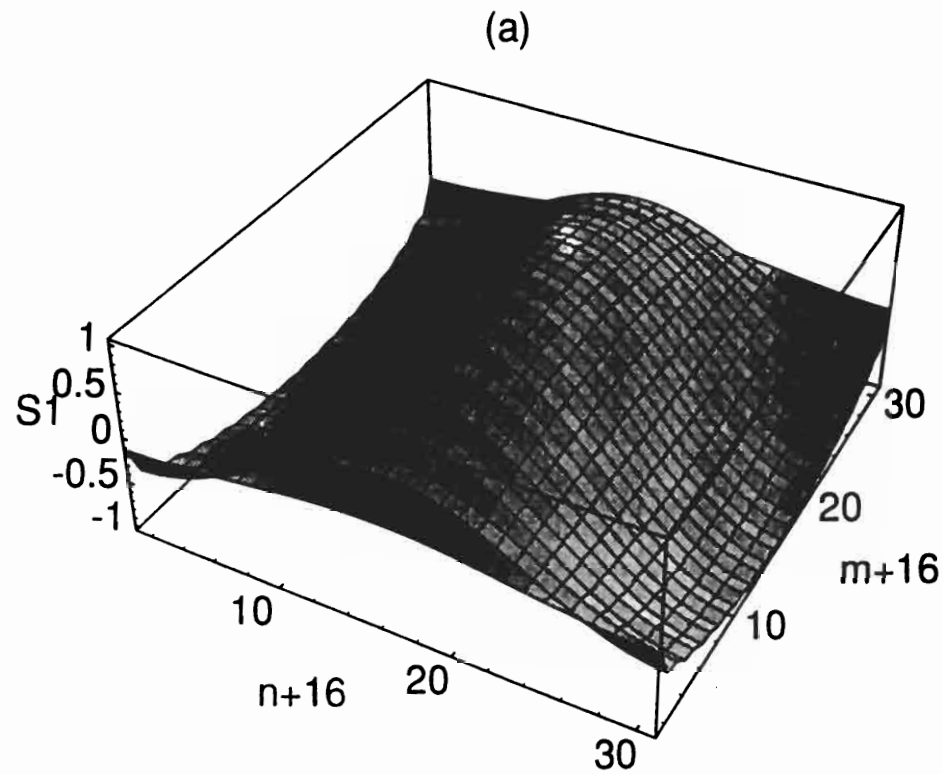
(a)
S1
1
0.5
0
-0.5
-1
10
n+16
20
30
30
20
m+16
10

Fig. 2

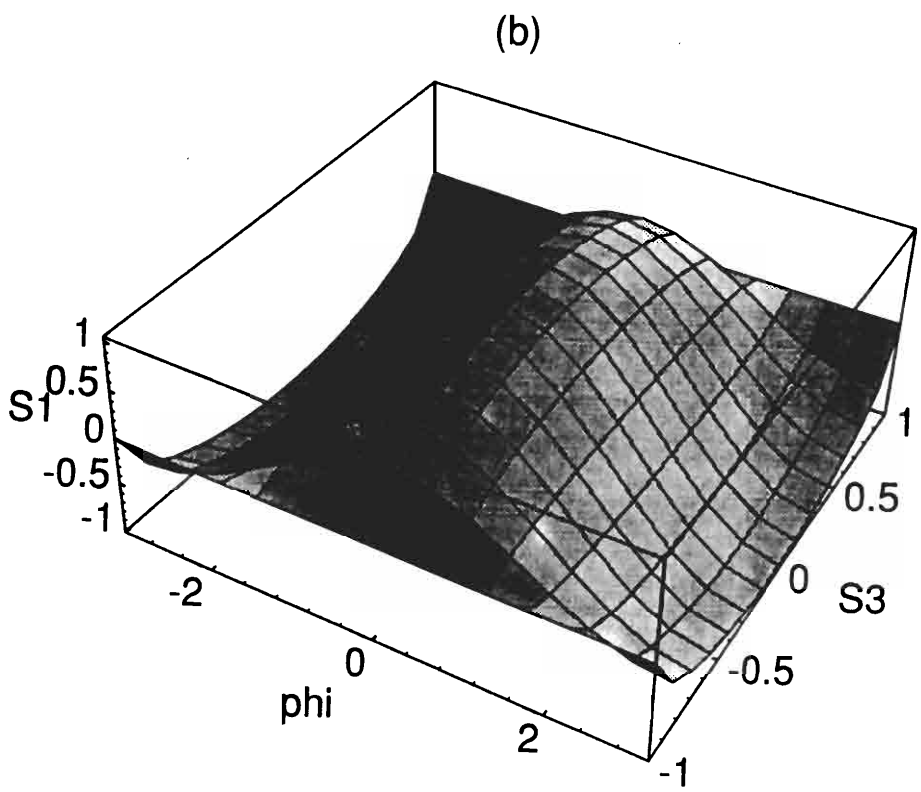

Fig. 2

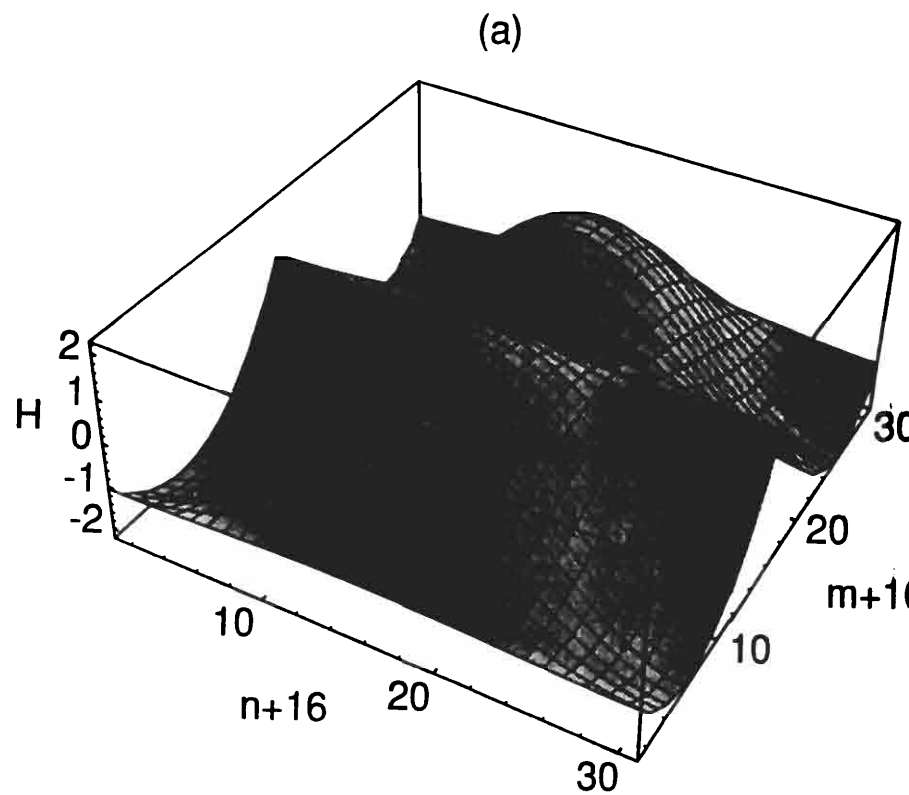

Fig. 3

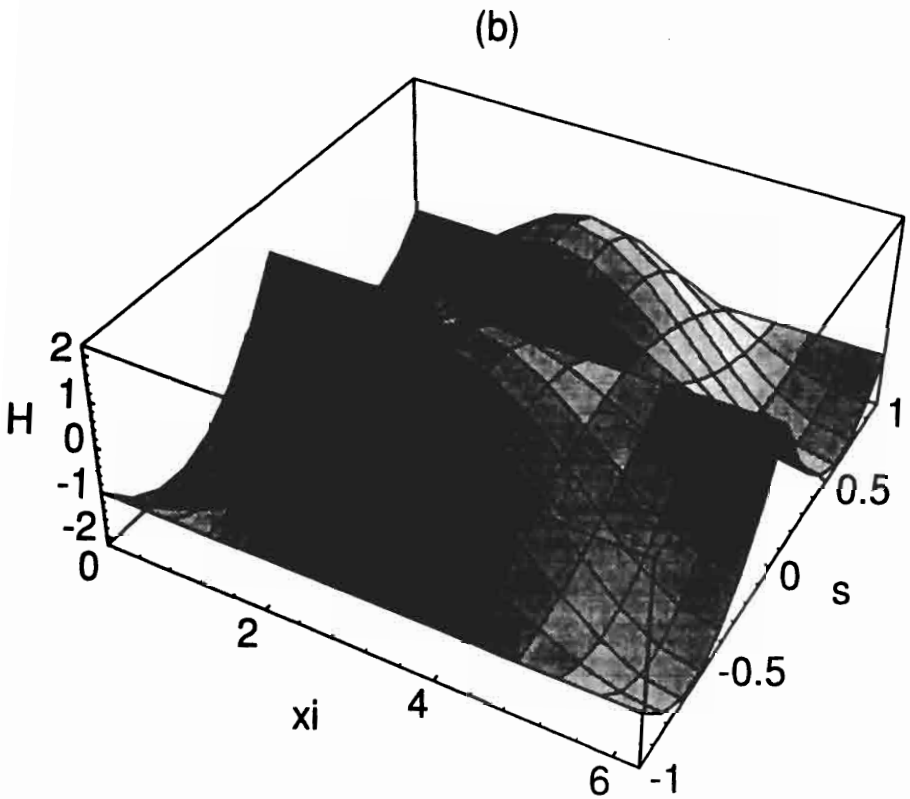
(b)
H
2
1
0
-1
-2
0
2
4
6
xi
1
0.5
0
-0.5
-1
s

Fig. 3

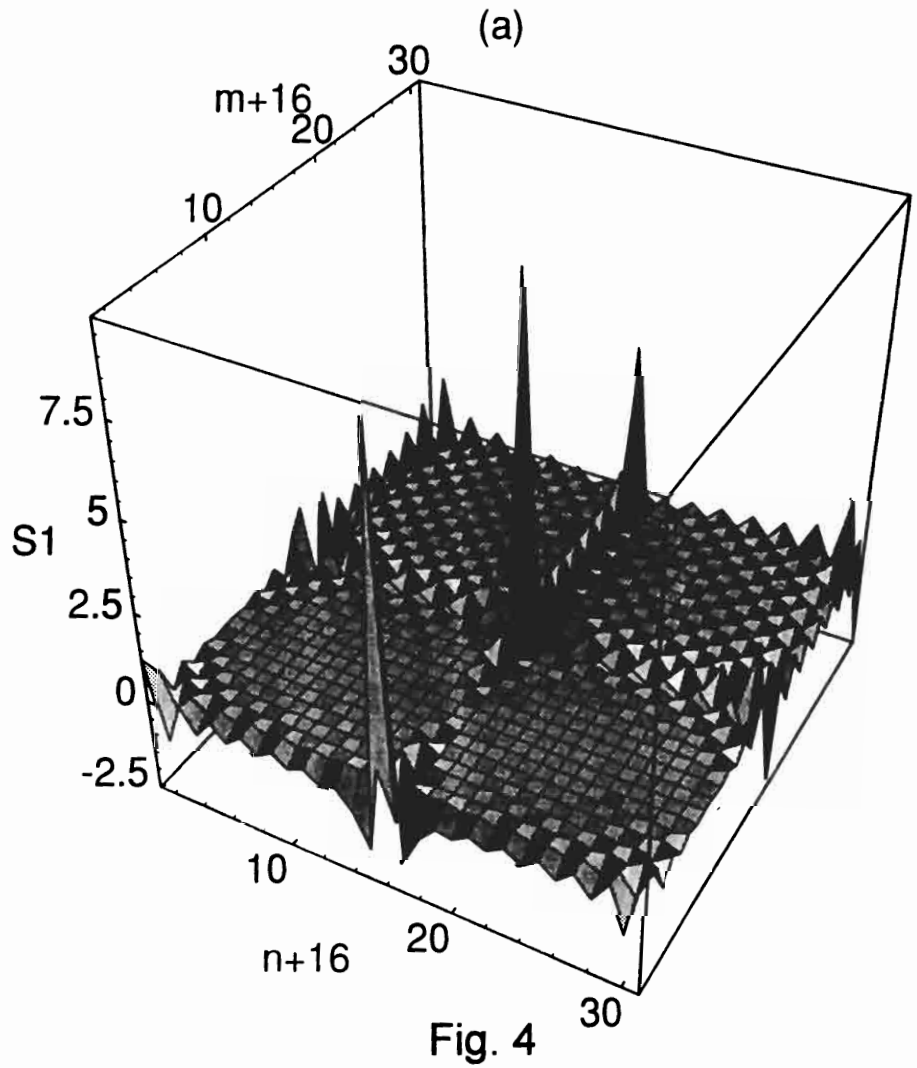
(a)
S1
7.5
5
2.5
0
-2.5
10
20
30
m+16
10
20
30
n+16

Fig. 4

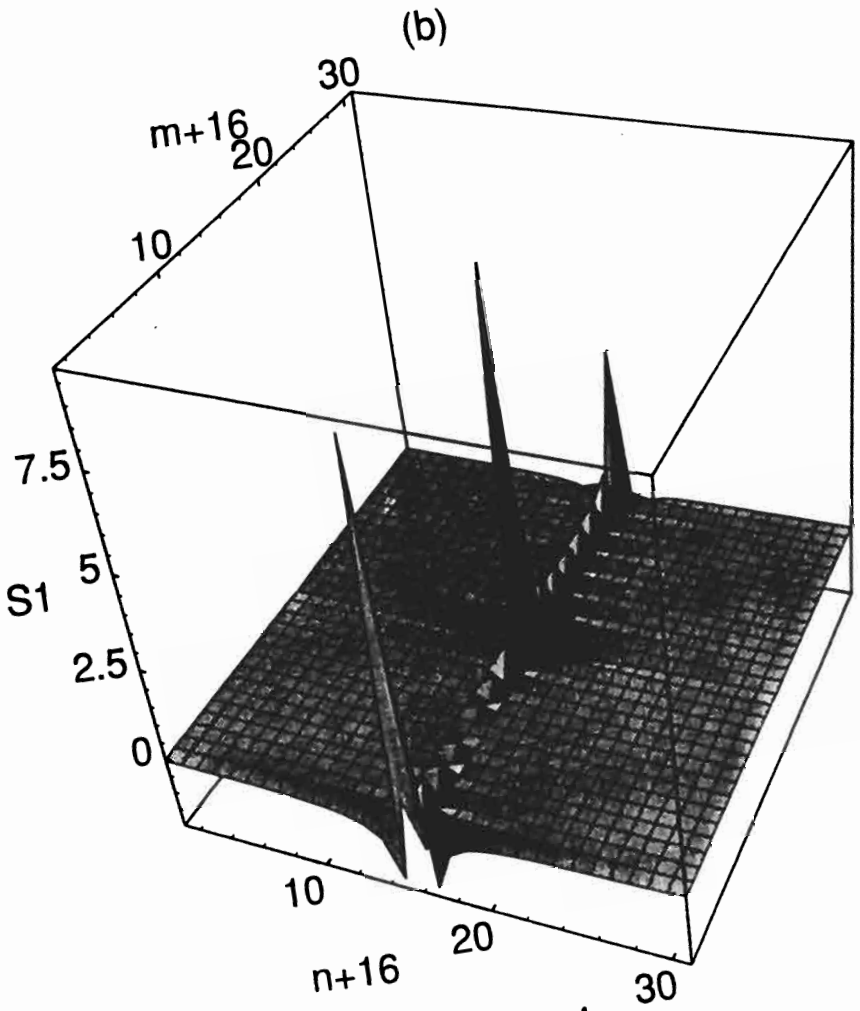
(b)
m+16
30
20
10
7.5
S1
5
2.5
0
10
20
30
n+16

Fig. 4

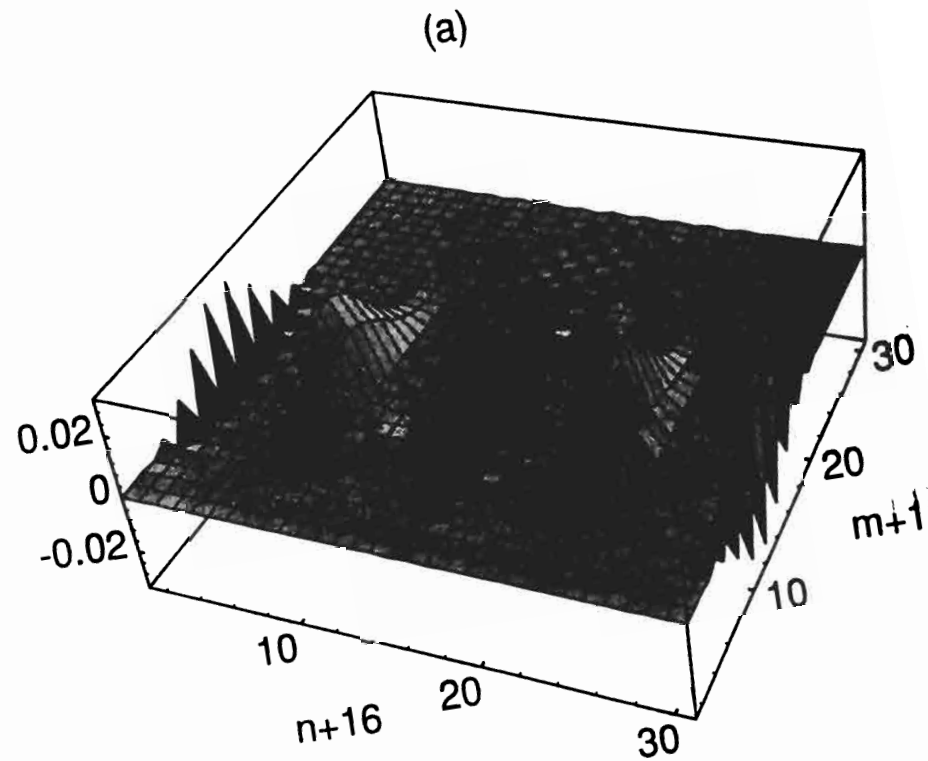
(a)
0.02
0
-0.02
10
20
30
n+16
30
20
10

Fig. 5

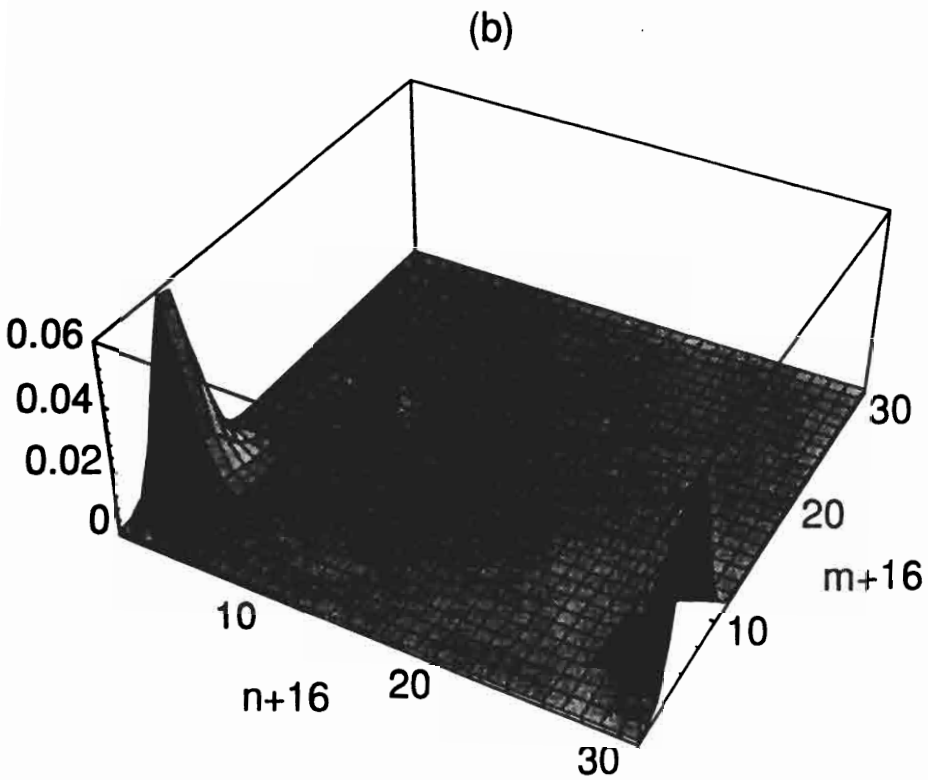
(b)
0.06
0.04
0.02
0
10
n+16
20
30
10
20
30
m+16

Fig. 5

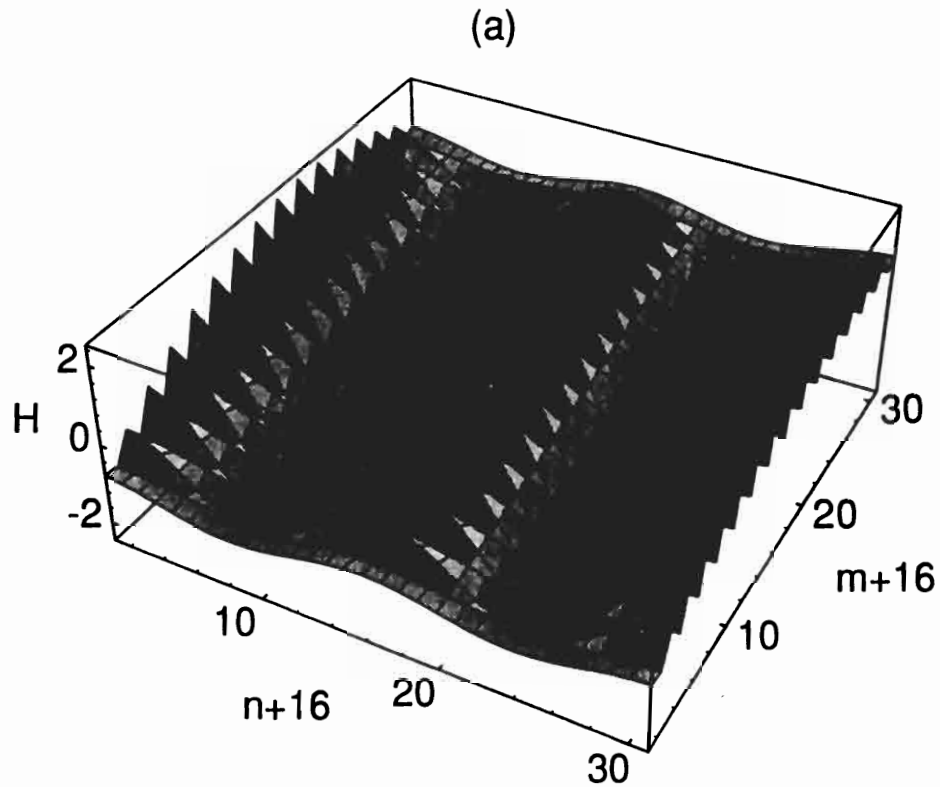
(a)
2
H
0
-2
10
n+16
20
30
10
20
30
m+16

Fig. 6

(b)

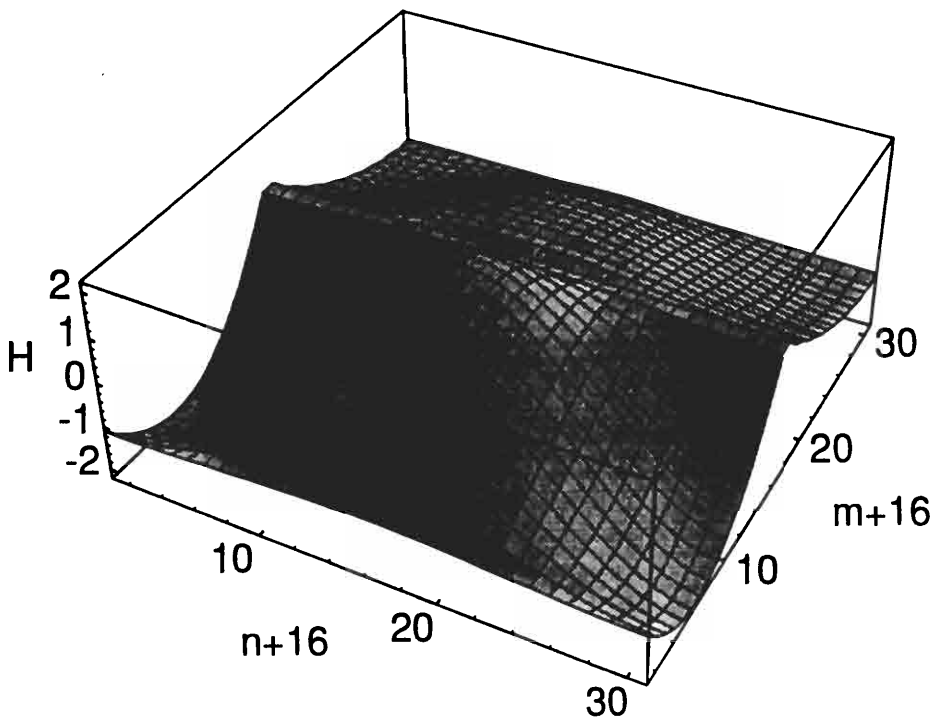

Fig. 6